

Transition to chaos in a V-shaped cavity heated from below

S. Bhowmick and F. Xu

Department of Mechanics
Beijing Jiaotong University, Beijing 100044, China

Abstract

The bottom of a river is usually hot owing to the presence of various plants and in turn natural convection flows occur in a river. In this study, the transition of natural convection flows in the V-shaped cavity heated from below is numerically investigated. A wide range of Rayleigh numbers from 10^0 to 10^6 , the Prandtl number of 7 and the aspect ratio of 0.5 is considered. Numerical results show that a sequence of bifurcations may occur as the Rayleigh number increases, including a pitchfork bifurcation from a symmetrical to an asymmetrical state and a Hopf bifurcation from a steady to an unsteady state. The critical Rayleigh numbers for different bifurcations are obtained based on a great number of numerical tests. The spectral analysis is also employed to study the oscillations of natural convection flows in the cavity and the fundamental frequency is obtained.

Introduction

Natural convection is common in nature and thus has received increasing attention. In particular, natural convection in a cavity has been investigated by many investigators owing to the simple geometry [1]. Natural convection in the cavity usually involves two scenarios for which the cavity is imposed by a vertical temperature gradient or by a horizontal temperature gradient. One of the earliest studies of natural convection in the cavity imposed by a horizontal temperature difference was reported in [1], which demonstrated that the mode of heat transfer is primarily dominated by conduction for sufficiently small Rayleigh numbers. However, natural convection flows are dominated by convection if the Rayleigh number exceeds the critical value. Natural convection flows at the primary symmetric state in the cavity are induced through the viscous shear by the baroclinity [2]. The thermal boundary layer adjacent to the vertical wall is steady for small Rayleigh numbers, but distinct travelling waves appear in the thermal boundary layer owing to convective instability for sufficiently large Rayleigh numbers [3]. Apart from natural convection flows driven by the baroclinity, natural convection flows induced by a vertical temperature difference (Rayleigh-Bénard instability) are also extensively present and considerably studied [4]. Particularly, turbulent Rayleigh-Bénard convection in the cavity is recently focused by increasing investigators (see e.g., [5]).

A square or rectangular cavity is not an adequate model for many industrial systems and geophysical situations in which the cavity geometry varies or involves one or more inclined walls. Natural convection flows on an inclined surface, termed as ‘anabatic flow’ or ‘katabatic flow’, are also common in nature such as in a valley [6]. Naturally, natural convection flows in a cavity with one or more inclined walls have been increasingly studied owing to their wide presence [7]. In fact, natural convection flows in a triangular cavity are an important extension of Rayleigh-Bénard convection [8]. Therefore, the dynamics and heat transfer of natural convection flows in an attic-shaped cavity imposed by an inverse temperature gradient are investigated in previous studies [9,10]. The transition from symmetric to asymmetric

flow is discussed in [11] in which a Pitchfork bifurcation is characterized with the increase of the Grashof number and validated by the experimental data. Recently, transient natural convection flows in the attic-shaped cavity have also been visualized in [12]. The development of transient flows following sudden heating and cooling is classified into three distinct stages: an initial stage, a transitional stage, and a steady or quasi-steady stage.

Natural convection flows of initially stratified fluid in a V-shaped cavity are investigated by few researchers [8,13]. Their intention is aimed at understanding of the mechanism for appearance and disappearance of fog in a valley. The experiment in [8] visualizes the breakup of the stratified structure in a V-shaped water tank in which two flow configurations are described. Recently, Bhowmick et al. [13] also observed natural convection flows of the initially stratified fluid in the cavity suddenly heated from below. The intrusion flow is discharged from the mid height of the cavity at which the temperature is the same as that of the inclined wall. In the early time of the transitional stage, the flow becomes chaotic for large Rayleigh numbers. Stratification is completely destroyed with the increase of time and finally the temperature of the fluid in the whole cavity becomes uniform. Additionally, turbulent natural convection flows in the V-shaped cavity have also been investigated and heat transfer through the cavity is calculated in [14].

The literature review shows that there are few studies of natural convection flows in a V-shaped cavity [8,13,14]. However, the study of natural convection flows in the V-shaped cavity is of significance owing to their extensive presence in nature and industrial systems [14]. In particular, the transition to a chaotic flow in the cavity heated from below is still indistinct, which motivates this study. In the present study, the transitional flow in the V-shaped cavity is investigated using two dimensional numerical simulation. A sequence of bifurcations in the transition from steady to chaotic state is described. The transition involves a Pitchfork bifurcation from symmetric to asymmetric state, then a set of further bifurcations at asymmetric steady state, a Hopf bifurcation from steady to unsteady state, and a bifurcation from periodic to chaotic state.

Model and numerical procedures

In this study, natural convection in a V-shaped cavity is investigated using two dimensional numerical simulation. That is, the development of natural convection in the cavity is governed by the two-dimensional Navier-Stokes with the Boussinesq approximation and energy equations. The non-dimensional format of governing equations can be expressed as [13]:

$$\frac{\partial u}{\partial x} + \frac{\partial v}{\partial y} = 0, \quad (1)$$

$$\frac{\partial u}{\partial \tau} + u \frac{\partial u}{\partial x} + v \frac{\partial u}{\partial y} = -\frac{\partial p}{\partial x} + \frac{\text{Pr}}{\text{Ra}^{1/2}} \left(\frac{\partial^2 u}{\partial x^2} + \frac{\partial^2 u}{\partial y^2} \right), \quad (2)$$

$$\frac{\partial v}{\partial \tau} + u \frac{\partial v}{\partial x} + v \frac{\partial v}{\partial y} = -\frac{\partial p}{\partial y} + \frac{\text{Pr}}{\text{Ra}^{1/2}} \left(\frac{\partial^2 v}{\partial x^2} + \frac{\partial^2 v}{\partial y^2} \right) + \text{Pr} \theta, \quad (3)$$

$$\frac{\partial \theta}{\partial \tau} + u \frac{\partial \theta}{\partial x} + v \frac{\partial \theta}{\partial y} = \frac{1}{\text{Ra}^{1/2}} \left(\frac{\partial^2 \theta}{\partial x^2} + \frac{\partial^2 \theta}{\partial y^2} \right). \quad (4)$$

Here, the governing parameters are the Prandtl number (Pr), the Rayleigh number (Ra) and the aspect ratio (A), expressed as:

$$\text{Pr} = \frac{\nu}{\kappa}, \text{Ra} = \frac{g\beta(T_h - T_c)H^3}{\nu\kappa}, A = \frac{H}{L}. \quad (5)$$

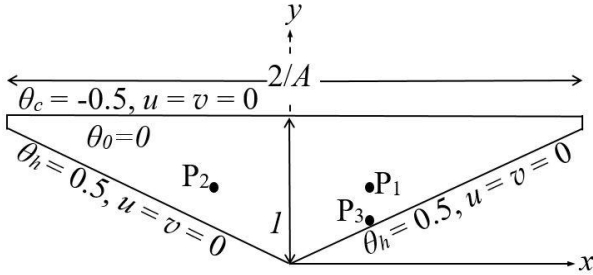


Figure 1. Domain and boundary conditions with the monitoring points P1 (0.5, 0.5), P2 (-0.5, 0.5), P4 (0.5, 0.255), which are used in the subsequent figures.

The physical model and boundary conditions are illustrated in figure 1. To compare the results with the experimental results in [8], we consider the similar dimensions of the cavity including the aspect ratio of $A = 0.36$. The miniscule tips were cut from the both top corners (4% of $1/A$) to eliminate the singularity at the section part between the top and inclined walls. The studies [13,14] indicate that the slight modification has no influence on the fluid flow and heat transfer. The top and the bottom wall are cooled and heated, respectively, but the two tips of the cavity are considered to be adiabatic. No-slip boundary condition is assigned to all boundaries. At the initial time, the fluid in the cavity is motionless and isothermal.

In this study, a finite volume method was used to discretize the Navier-Stokes equations. We discretized the advection terms using the QUICK scheme [13]. The viscous terms were discretized using a second-order central difference, and the unsteady terms using a second-order implicit time-marching method.

Grid dependence tests were carried out between different non-uniform meshes with finer grids in the neighborhood of all borders and coarser grids in the internal region. The mesh of 800×150 was used for all numerical cases in this study. In addition, the time step of $\Delta\tau = 0.0025$ is selected after time step dependence tests.

Results

For understanding of the transition to an unsteady flow in a V-shaped cavity heated from the inclined wall and cooled from the top wall, two dimensional numerical simulation is carried out for $\text{Ra} = 10^0$ to 10^6 , $\text{Pr} = 7.0$ and $A = 0.5$ in this study. Numerical results show that a set of bifurcations occurs in the transition from a conduction dominated symmetric steady flow for small Rayleigh numbers to an unsteady flow for large Rayleigh numbers. A typical symmetric steady flow for $\text{Ra} \leq 1.3 \times 10^4$, an asymmetric steady flow for $1.4 \times 10^4 \leq \text{Ra} \leq 1.6 \times 10^5$, a periodic flow for $1.7 \times 10^5 \leq \text{Ra} \leq 2.6 \times 10^5$ and a chaotic flow for $\text{Ra} \geq 2.7 \times 10^5$ are described in the following sections.

Figure 2 shows isotherms and streamlines around $\text{Ra} = 10^4$. Figure 2(a) shows that the flow is symmetric for $\text{Ra} = 10^4$. However, the flow becomes asymmetric for $\text{Ra} = 3 \times 10^4$, as illustrated in figures 2(b) and 2(c). Clearly, one of cells can become larger and move towards the left in figure 2(b) or to the right in figure 2(c), which depends on initial perturbations. This means that the symmetry of the flow structure is broken between $\text{Ra} = 10^4$ and 3×10^4 . In fact, the transition from symmetric to asymmetric state is a supercritical Pitchfork bifurcation, which is a result of the onset of Rayleigh-Bénard instability, referred to e.g., [15] for details of bifurcation. In addition, apart from the symmetric break, the number of cells in the cavity increases with the Rayleigh number. For example, there are four cells for $\text{Ra} = 10^4$ in figure 2(a) but six cells for $\text{Ra} = 3 \times 10^4$ in figures 2(b) and 2(c). This also implies that further bifurcations occurs with the increase of the Rayleigh number.

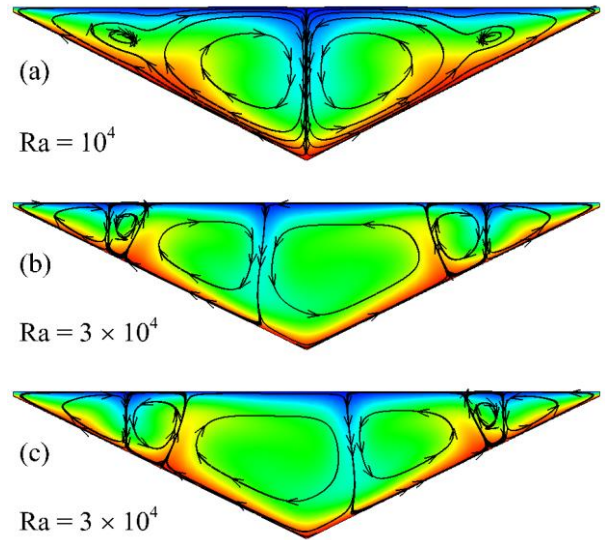


Figure 2. Isotherms and streamlines in the cavity for different Rayleigh number.

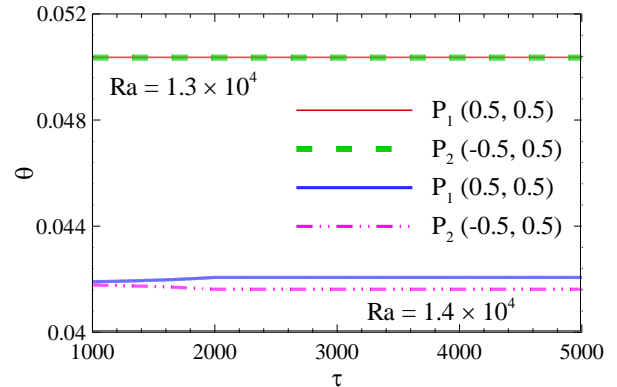


Figure 3. Time series of the temperature at the points P1 and P2 in the fully developed stage for different Rayleigh numbers.

For confirmation of the critical Rayleigh number for which a Pitchfork bifurcation occurs, figure 3 shows time series of the temperatures at the two points P1 (0.5, 0.5) and P2 (-0.5, 0.5), which are symmetric respect to the y -axis. Clearly, as time increases, temperature time series at the two points are the same for $\text{Ra} = 1.3 \times 10^4$ (still the same at a larger time based on the further examination of numerical results) but become different for $\text{Ra} = 1.4 \times 10^4$. This means that a transition from a symmetric to an asymmetric temperature distribution occurs between $\text{Ra} = 1.3 \times 10^4$ and 1.4×10^4 . In fact, the flow in the

cavity is driven by only the baroclinity induced by the inclined wall for $Ra \leq 1.3 \times 10^4$ but by both the baroclinity and the Rayleigh-Bénard convection for $Ra \geq 1.4 \times 10^4$. This implies that the dynamics also changes in the pitchfork bifurcation around $Ra = 1.4 \times 10^4$.

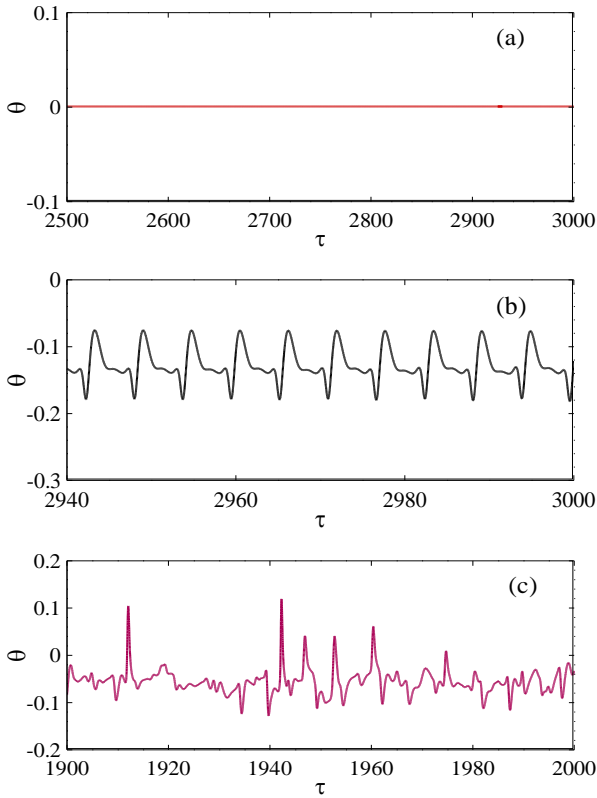


Figure 4. Time series of the temperature at the point P3 in the fully developed stage for different Rayleigh numbers. (a) $Ra = 1.6 \times 10^5$. (b) $Ra = 1.7 \times 10^5$. (c) $Ra = 10^6$.

To further understand the unsteady flow for large Rayleigh numbers, temperature time series were monitored and analysed. Figure 4 shows temperature time series for different Rayleigh numbers. Clearly, the flow in the fully developed stage is steady for $Ra = 1.6 \times 10^5$ in figure 4(a) but periodic for $Ra = 1.7 \times 10^5$ in figure 4(b). This is a Hopf bifurcation from steady to periodic state. As the Rayleigh number increases, the flow can become chaotic in the fully developed stage, as shown in in figure 4(c). The spectral analysis was also performed for different Rayleigh numbers. The results show that the fundamental frequency of the periodic flow is 0.28 with harmonic modes for $Ra = 1.6 \times 10^5$. The examination of numerical results shows that the fundamental frequency varies for different Rayleigh numbers.

Additionally, the largest Lyapunov exponent was calculated for different Rayleigh numbers (also see [16]). The study [16] indicates that the largest Lyapunov exponent (λ_L) is positive when a nonlinear system is chaotic. The transition from order to chaos can be characterized by the largest Lyapunov exponent. Figure 5 shows the largest Lyapunov exponent for different Rayleigh numbers. It is clear that the largest Lyapunov exponent is not positive for $Ra \leq 2.6 \times 10^5$. However, the largest Lyapunov exponent significantly increases for $Ra \geq 2.7 \times 10^5$ at which $\lambda_L = 0.000629$. This implies that the unsteady flow in the cavity becomes chaotic for $Ra \geq 2.7 \times 10^5$, which is consistent with that in figure 4. As the Rayleigh number increases further, the largest Lyapunov exponent continuously increases and thus the unsteady flow becomes more chaotic, as shown in figure 4.

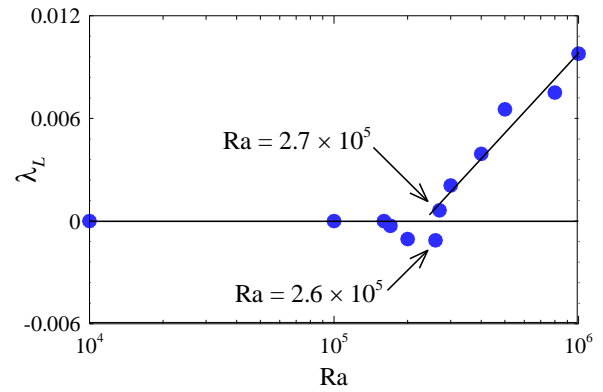


Figure 5 Dependence of the largest Lyapunov exponent on the Rayleigh number.

To understand heat transfer in the cavity, figure 6 shows the dependence of the Nusselt number on the Rayleigh number. It is seen from this figure that the scaling of $Nu \sim Ra^{1/4}$ works for the present range of Rayleigh numbers, although Nu slightly decreases as the Rayleigh number increases. That is, the scaling of $Nu \sim Ra^{1/4}$ can quantify heat transfer for the present Rayleigh numbers.

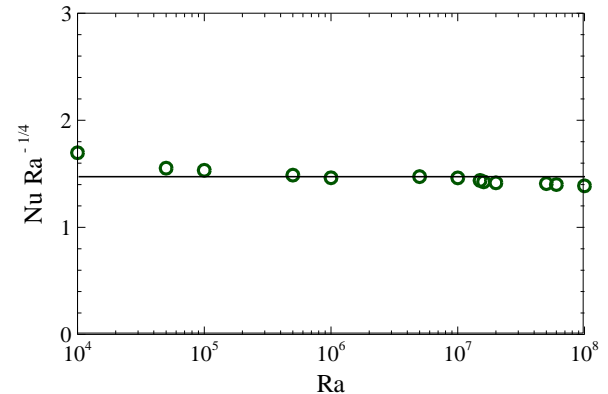


Figure 6 Dependence of the Nusselt number on the Rayleigh number.

Conclusions

In this study, two-dimensional numerical simulation is used to investigate natural convection flows in a V-shaped cavity heated from the inclined wall and cooled from the top wall. An extensive range of Rayleigh numbers from 10^0 to 10^6 is considered for $Pr = 7.0$ and $A = 0.5$. Different flow structures in the cavity are described.

It is demonstrated that the transition of natural convection flows goes through a sequence of bifurcations from a symmetric steady state to an unsteady state. Natural convection flows in the cavity are steady and symmetric for $Ra \leq 1.3 \times 10^4$, which are also driven by the baroclinity generated by the thermal inclined wall through viscous shear. A Pitchfork bifurcation from symmetric to asymmetric state occurs for $1.3 \times 10^4 \leq Ra \leq 1.4 \times 10^4$. As the Rayleigh number increases, a sequence of bifurcations occurs with the increase in the number of cells. A Hopf bifurcation from steady to periodic state occurs for $1.6 \times 10^5 \leq Ra \leq 1.7 \times 10^5$. That is, natural convection flows in the cavity are periodic for $Ra = 1.7 \times 10^5$ to 2.6×10^5 but chaotic for $Ra \geq 2.7 \times 10^5$.

In addition, the 3D numerical simulation and the experiment corresponding to the current numerical simulation is on the way.

References

- [1] Batchelor, G.K., Heat transfer by free convection across a closed cavity between vertical boundaries at different temperatures, *Quart. Appl. Math.*, **12**, 1954, 209-233.
- [2] Gill, A.E., The boundary-layer regime for convection in a rectangular cavity, *J. Fluid Mech.*, **26**, 1966, 515-536.
- [3] Patterson, J.C. & Imberger, J., Unsteady natural convection in a rectangular cavity, *J. Fluid Mech.*, **100**, 1980, 65-86.
- [4] Manneville, P., Rayleigh-Bénard convection: Thirty years of experimental, theoretical, and modeling work, in *Dynamics of Spatio-Temporal Cellular Structures: Henri Bénard Centenary Review*, editors I. Mutabazi, J. Wesfreid and E. Guyon, Springer, 2006, 41-65.
- [5] De, A.K., Eswaran, V. & Mishra, P.K., Scalings of heat transport and energy spectra of turbulent Rayleigh-Bénard convection in a large-aspect-ratio box, *Int. J. Heat Fluid Flow*, **67**, 2017, 111-124.
- [6] Prandtl, L., *Essentials of Fluid Dynamics*, Blackie, London, 1952.
- [7] Lehner, M. & Gohm, A., Idealised simulations of daytime pollution transport in a steep valley and its sensitivity to thermal stratification and surface albedo, *Bound. Lay. Meteorol.*, **134**, 2010, 327-351.
- [8] Princevac, M. & Fernando, H.J.S., Morning breakup of cold pools in complex terrain, *J. Fluid Mech.*, **616**, 2008, 99-109.
- [9] Saha, S.C. & Khan, M.M.K., A review of natural convection and heat transfer in attic-shaped space, *Energ. Buildings*, **43**, 2011, 2564-2571.
- [10] Poulidakos, D. & Bejan, A., The fluid dynamics of an attic space, *J. Fluid Mech.*, **131**, 1983, 251-269.
- [11] Holtzman, G.A., Hill, R.W. & Ball, K.S., Laminar natural convection in isosceles triangular enclosures heated from below and symmetrically cooled from above, *J. Heat Transfer*, **122**, 2000, 485-491.
- [12] Lei, C., Armfield, S. & Patterson, J.C., Unsteady natural convection in a water-filled isosceles triangular enclosure heated from below, *Int. J. Heat Mass Transfer*, **51**, 2008, 2637-2650.
- [13] Bhowmick, S., Xu, F., Zhang, X. & Saha, S.C., Natural convection and heat transfer in a valley shaped cavity filled with initially stratified water, *Int. J. Therm. Sci.*, **128**, 2018, 59-69.
- [14] Kenjeres, S., Heat transfer enhancement induced by wall inclination in turbulent thermal convection, *Phys. Rev. E*, **92**, 2015, 053006.
- [15] Drazin, P.G., *Introduction to hydrodynamic stability*, Cambridge University Press, Cambridge, 2002.
- [16] Jimenez, J., Transition to turbulence in two-dimensional Poiseuille flow, *J. Fluid Mech.*, **218**, 1990, 265-297.